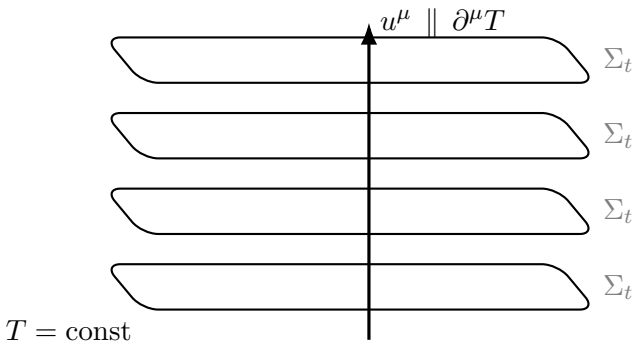

Figure 1: Preferred foliation by $T(x)$ with unit timelike u^μ normal to the leaves Σ_t.

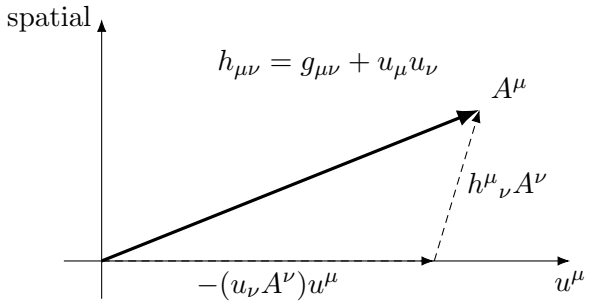

Figure 2: Any vector decomposes into temporal and spatial parts via the projector $h^\mu{}_\nu$.

2) Circulation quantization on a ring latex Copy code 3) Energy landscape for $\rightarrow$ R$\rightarrow$T latex Copy code 4) Preferred foliation and u

latex Copy code 5) Flux of = d H=dB through a surface pierced by a string latex Copy code

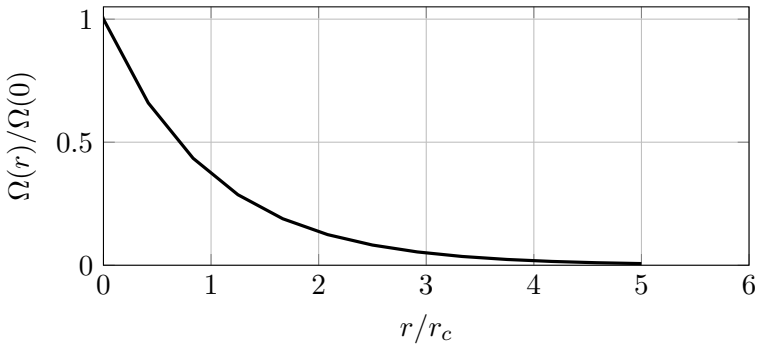

Figure 3: Canonical profile $\Omega(r) = \Omega(0)e^{-r/r_c}$.

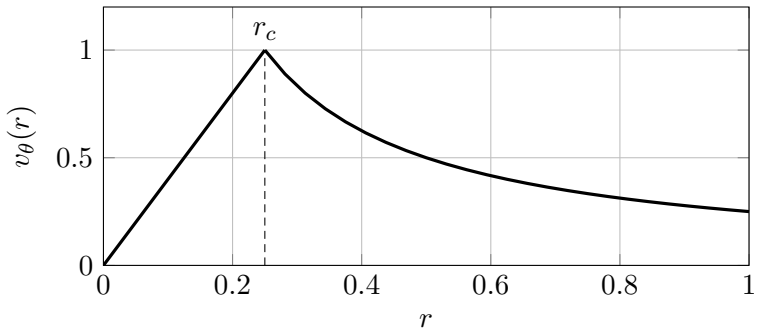

Figure 4: Rankine model: solid-body core ($v \propto r$) matched to irrotational shell ($v \propto 1/r$).

1) Mach–Zehnder Interferometer (SST view)

2) Knot invariants overlay on a trefoil (C(K)C(K)C(K), H(K)H(K)H(K))

3) Core profile (r)$\Omega(r)(r)andSwirlClockdtlocal/dtdt_{\mathrm{local}}/dt_{/dt}$

4) Fringe geometry (slit separation sss, distance LLL, screen coordinate xxx)

5) Polarization selection (helicity matching to trefoil chirality)

6) (Already supplied earlier) Visibility vs. which-way coupling V=eV=e$^{-\Gamma 2}V = e$

(Keep for completeness; no changes needed.)

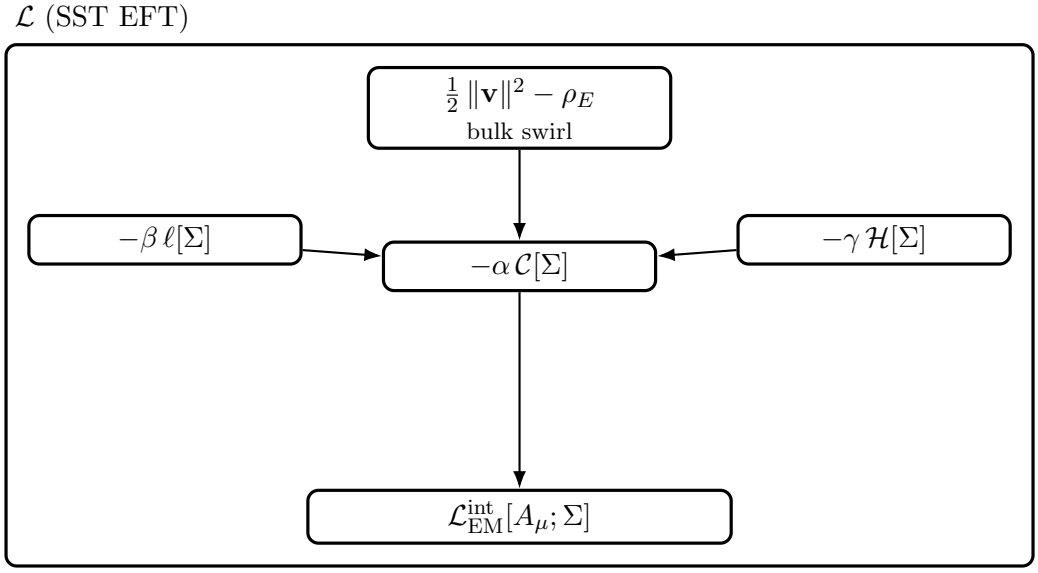

Figure 5: SST Lagrangian as modular terms.

7) (Optional EFT block diagram) Lagrangian terms as modules

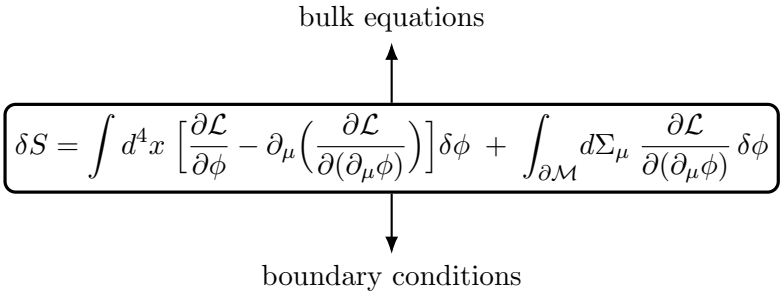

Figure 6: Variation of the action: Euler–Lagrange equations plus boundary term.

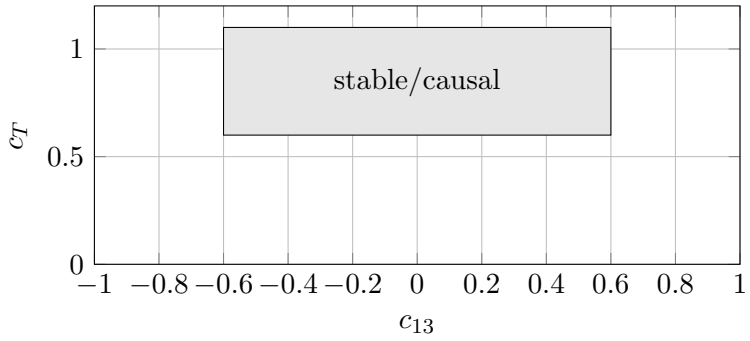

Figure 7: Illustrative stability/causality window in (c_{13}, c_T).

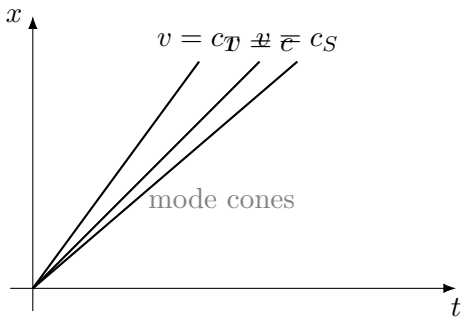

Figure 8: Linearized mode cones with different propagation speeds.

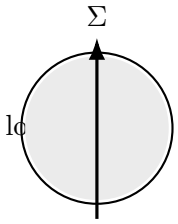

Figure 9: String loop and its worldsheet Σ (schematic).

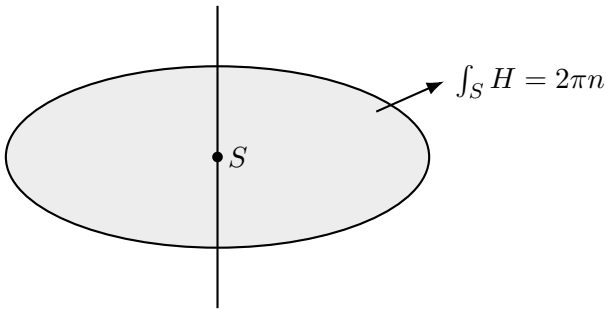

Figure 10: Worldsheet piercing a surface S, quantizing the H-flux.

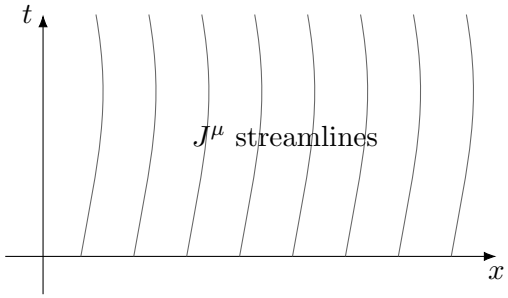

Figure 11: Schematic Noether current J^μ flowlines.

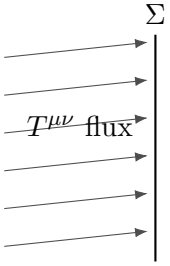

Figure 12: Energy–momentum flux crossing a surface element.

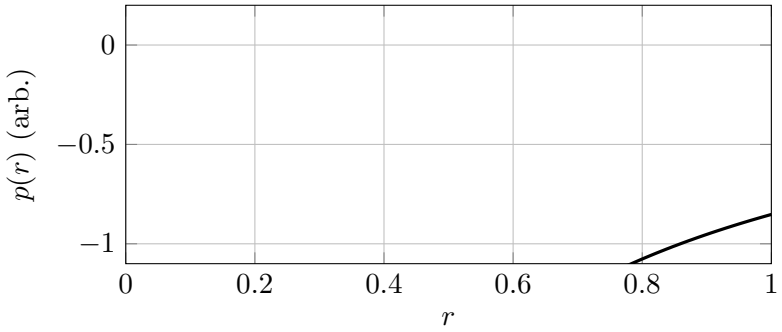

Figure 13: Qualitative pressure well induced by swirl.

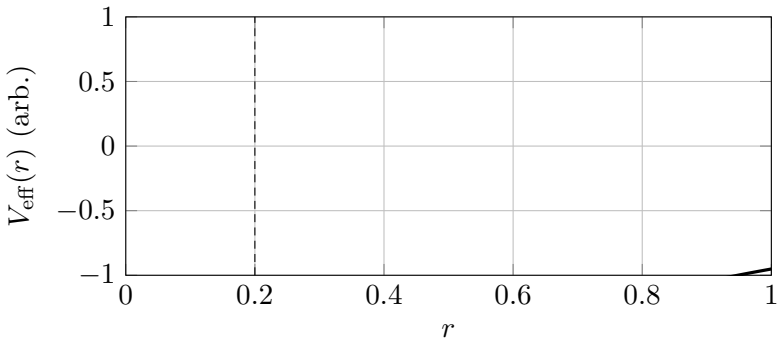

Figure 14: Effective potential with core scale r_c (schematic).

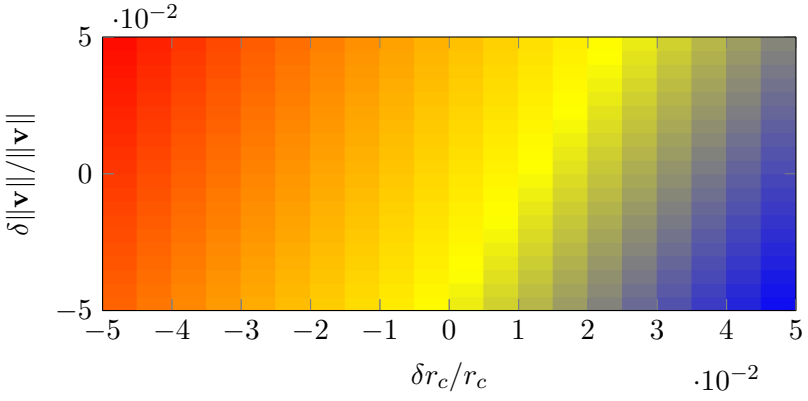

Figure 15: Illustrative relative change $\delta G/G$ vs. small parameter shifts (toy scaling).

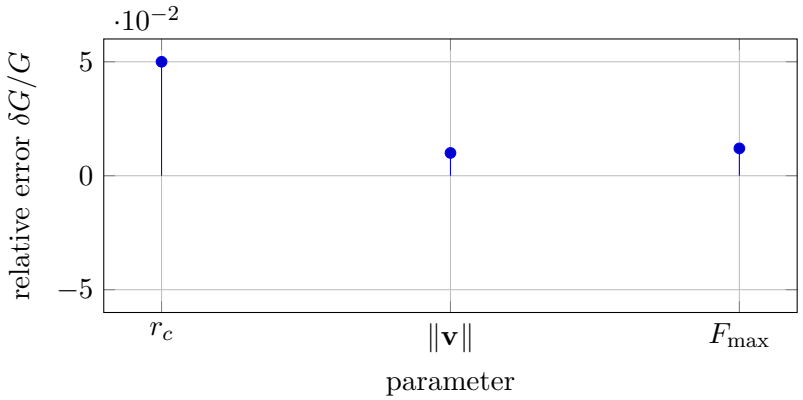

Figure 16: Toy sensitivity bars (edit with actual derivatives).

$\mathcal{R}$ (delocalized ring) $\mathcal{T}$ (localized knot)

Figure 17: Two-phase electron in SST: delocalized toroidal circulation $\mathcal{R}$ and localized knotted soliton $\mathcal{T}$.

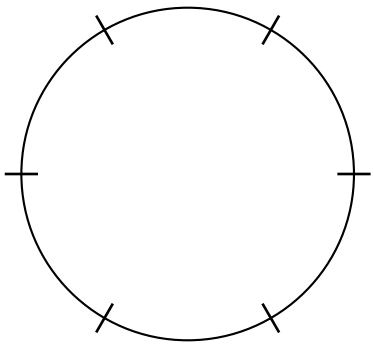

$$\Gamma_n = \oint v \cdot d\ell = n\frac{h}{m_e}, \quad \lambda_{\text{ring}} = \frac{2\pi R}{n} = \frac{h}{p_\theta}$$

Figure 18: Circulation quantization and de Broglie relation on the ring phase $\mathcal{R}$.

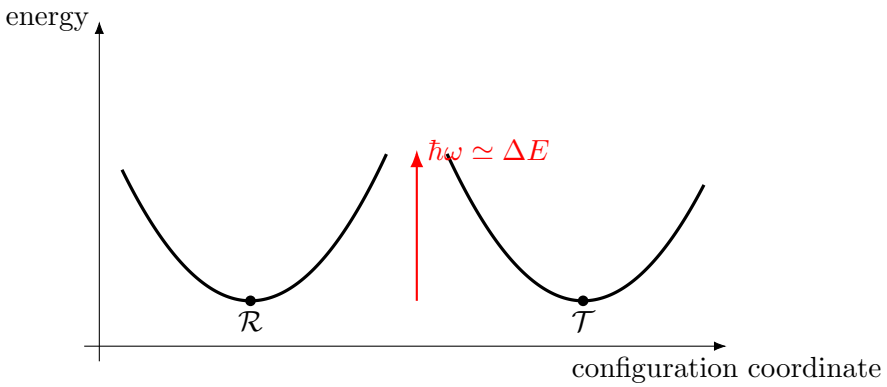

Figure 19: SST transition energy: $\Delta E = (\epsilon_0 A + \beta)\Delta L + \alpha C(\mathcal{T}) + \gamma \mathcal{H}(\mathcal{T})$.

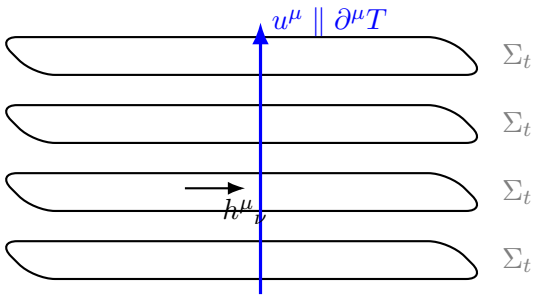

Figure 20: Preferred foliation by the clock field $T(x)$ with unit timelike u^μ, and spatial projector $h_{\mu\nu} = g_{\mu\nu} + u_\mu u_\nu$.

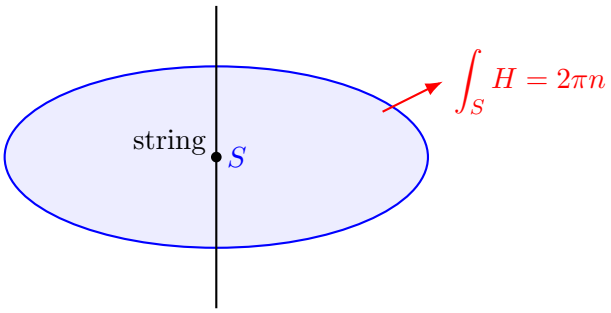

Figure 21: Worldsheet/flux cartoon: the swirl string pierces S, quantizing the H-flux.

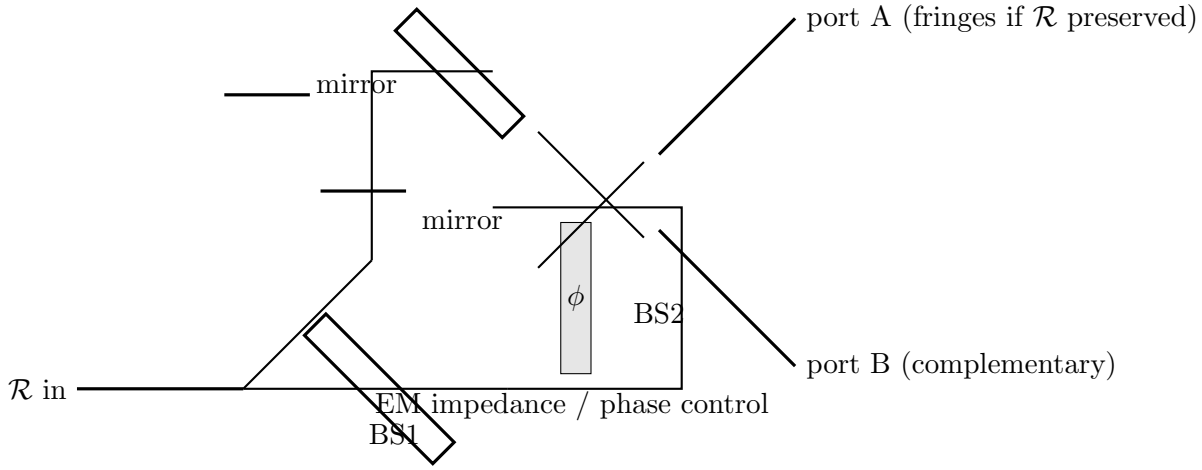

Figure 22: Mach–Zehnder in SST. The delocalized $\mathcal{R}$ phase splits/recombines; a phase/impedance element ϕ controls output fringes vs. which-way collapse to $\mathcal{T}$.

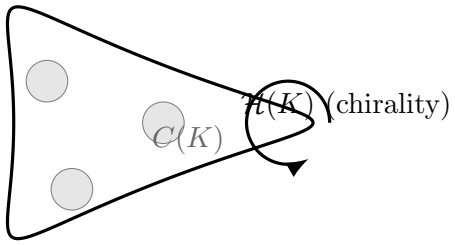

Figure 23: Trefoil schematic with overlays indicating near-contact regions ($C(K)$) and helicity/chirality cue ($\mathcal{H}(K)$).

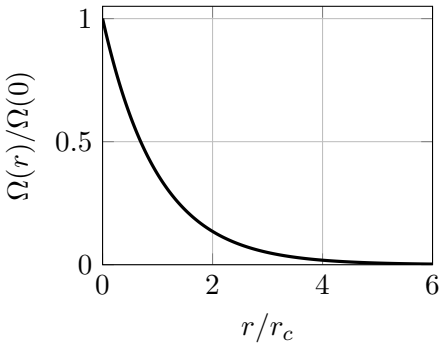

Figure 24: *
$\Omega(r) = \Omega(0)e^{-r/r_c}$.

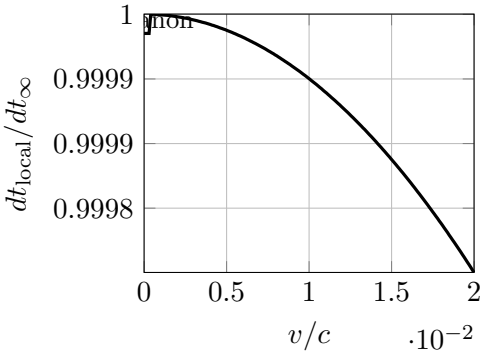

Figure 25: *
Swirl Clock: $\sqrt{1 - v^2/c^2}$, with canonical point marked.

Figure 26: Left: canonical angular profile. Right: local time rate vs. v/c.

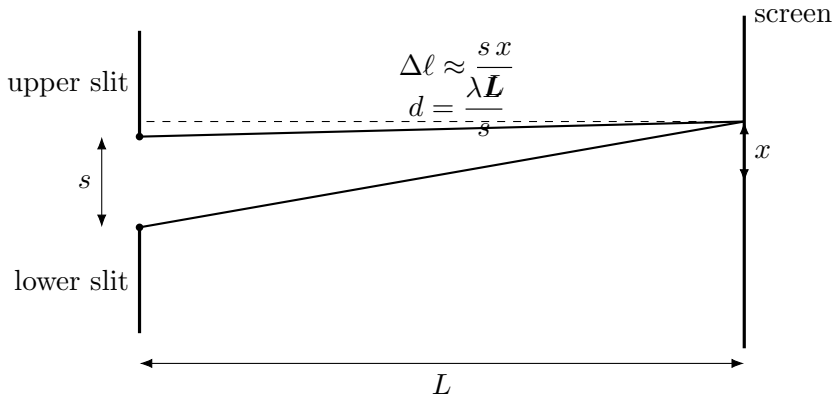

Figure 27: Double-slit geometry: path difference $\Delta\ell \approx s\,x/L$ and fringe spacing $d = \lambda L/s$.

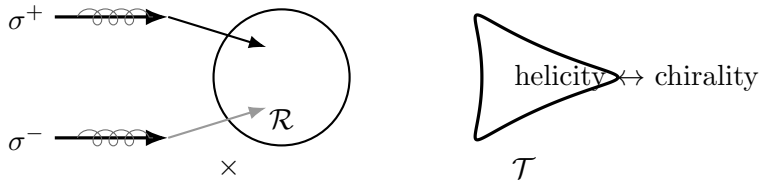

Figure 28: Helicity selection: circularly polarized light $\sigma^{\pm}$ couples preferentially to the chirality of the target knot $\mathcal{T}$, setting transition strength.

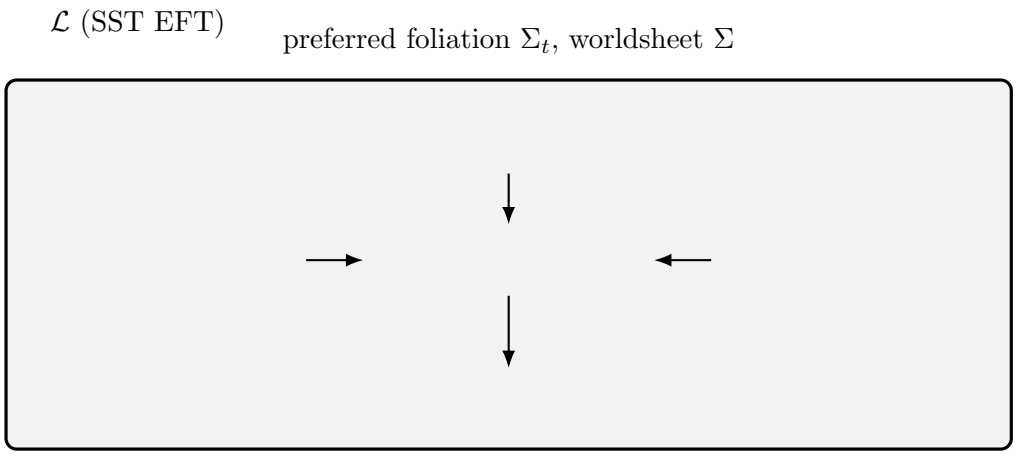

Figure 29: SST EFT ingredients as modular terms composing $\mathcal{L}$.